Supporting Information for

Schottky-barrier-free contacts with two-dimensional semiconductors by surface-engineered MXenes

Yuanyue Liu[1,2*], Hai Xiao[1], William A. Goddard III[1*]

[1]Materials and Process Simulation Center, [2]The Resnick Sustainability Institute
California Institute of Technology, Pasadena, California 91125, United States

*Email: yuanyue.liu.microman@gmail.com, wag@wag.caltech.edu

1. Stacking order of the group-6 MXenes

Material	Stacking order of the T, M, X, M, T layers
Cr_2C	ABC (no T layers)
Cr_2CO_2	ABABA
$Cr_2C(OH)_2$	ABCAB
Cr_2CF_2	ABCAB
Mo_2C	ABA (no T layers)
Mo_2CO_2	ABABA
$Mo_2C(OH)_2$	ABCBA
Mo_2CF_2	ABCBA

Table S1. The most stable stacking order of the group-6 MXenes

2. Electron density redistribution upon surface termination

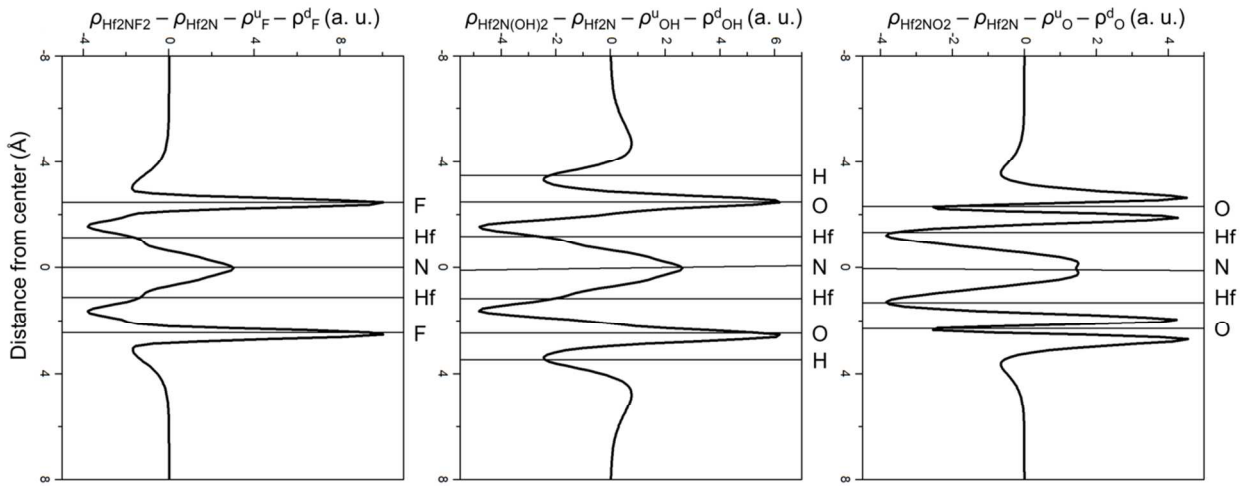

Figure S1. The electron density (averaged over the xy plane; arbitrary unit) of Hf_2NT_2, subtracted by the electron density of the isolated Hf_2N and the two T layers with the same coordinates as those in the Hf_2NF_2. This reflects the electron redistribution on Hf_2N and T after adsorption. Note that the change of the electron density is non-zero inside Hf_2N; both T and N layers become negatively charged while the surface Hf layers are positively charged.

3. Verification of SB-free contacts for electron/hole injection by the hybrid functional B3PW91

It is well established that hybrid functionals are superior to semilocal GGA functionals such as PBE for describing band gaps of semiconductors. Consequently we used the hybrid functional B3PW91, which we have shown to predict accurately both band gaps[1, 2] and band offsets[3], to validate the absence of SB's in two representative heterojunctions, $Hf_2N(OH)_2$-WSe_2 and Nb_2CO_2-WSe_2, for electron and hole injection, respectively.

The B3PW91 calculations were performed using the CRYSTAL14 package[4], which uses local atomic Gaussian-type basis sets. This enables fast evaluation of the Hartree-Fock exchange terms required for hybrid DFT method. We used the all-electron 6-311G(*d*) basis sets of triple-ζ quality for H, C, N and O, while for Se, Nb, Hf and W, we used the SBKJC relativistic effective core potentials and modified associated basis sets of triple-ζ quality. An extra-large grid, consisting of 75 radial points and 974 angular points, was used for accurate integration, and the reciprocal space was sampled by Γ-centered Monkhorst-Pack scheme[5] with 12×12×1 and 5×5×1 grids for $Hf_2N(OH)_2$-WSe_2 and Nb_2CO_2-WSe_2, respectively.

The B3PW91 results confirm that for the $Hf_2N(OH)_2$-WSe_2 case, the CBM of WSe_2 at the K point is below the Fermi level by 0.12 eV, i.e., electron injection from the $Hf_2N(OH)_2$ to the WSe_2 takes place spontaneously; for the Nb_2CO_2-WSe_2 case, the VBM of WSe_2 at the Γ point is above the Fermi level by 0.08 eV, i.e., hole injection from the Nb_2CO_2 to the WSe_2 takes place spontaneously.

4. The stability of O and OH termination of V_2C under applied potentials

To predict more accurately the electrochemical conditions for formation of $V_2C(OH)_2$, we used the Grand Canonical constant potential formulation with CANDLE implicit solvation model[6] as implemented in the jDFTx software[7-9] to perform explicit constant electrochemical potential (μ_e) calculations[42] using a $\sqrt{3}\times\sqrt{3}$ supercell of V_2C with various O/OH coverages, i.e., V_2CO_2, $V_2C(OH_{1/3})_2$, $V_2C(OH_{2/3})_2$ and $V_2C(OH)_2$. We used the GBRV ultrasoft pseudopotentials, with a plane wave cutoff of 544 eV (20 Hartree atomic units). The reciprocal space was sampled by Γ-centered Monkhorst-Pack scheme with an 8×8×1 grid. The ionic screening of net charges resulting from the constant μ_e condition was achieved with cation (0.1 M Na^+) and anion (0.1 M Cl^-) components in the fluid model under the JDFT framework. The algorithm employed by JDFTx variationally minimizes the grand canonical free energy at fixed electron chemical potential with respect to Kohn-Sham orbitals, fluid bound charge and an auxiliary Hamiltonian for the occupations. Previously we have found that the relative free energies are linearly dependent on the applied potential U for |U| < ~2 V (vs standard hydrogen electrode (SHE))[10], so we assume the U-dependence of free energy is linear between U = 0.0 and −1.2 V.

Zero-point energies (ZPE), enthalpy and entropy contributions to the free energies of $V_2C(OH_x)_2$ at room temperature (298.15 K) were calculated from vibrational modes of O/OH surface termi-

nation. The formation free energies of surface OH by electrochemical reduction using $H^+(H_3O^+/H_2O) + e^-$ were referenced to the free energy of $H_2(g)$, which was calculated including the translational and rotational contributions assuming the ideal gas model, in addition to the vibrational contributions..

System	ZPE	$(H - TS)_{vib(,rot,trans)}$
$H_2(g)$	0.2666	-0.3131
$V_2C(OH_{1/3})_2$	0.1958	-0.0024
$V_2C(OH_{2/3})_2$	0.3892	-0.0054
$V_2C(OH)_2$	0.5550	-0.0111

Table S2. The calculated enthalpy (H) and entropy (S) contributions (in eV) to the free energies of $V_2C(OH_x)_2$ (normalized to per formula unit) at room temperature (T = 298.15 K).

Our results (Figure S2) allow us to conclude that the full surface OH coverage of V_2C can be achieved by applying potentials under −0.5 V. This suggests that the desired $V_2C(OH)_2$ can be synthesized by applying a potential more negative than -0.5 V to a solution containing proton sources.

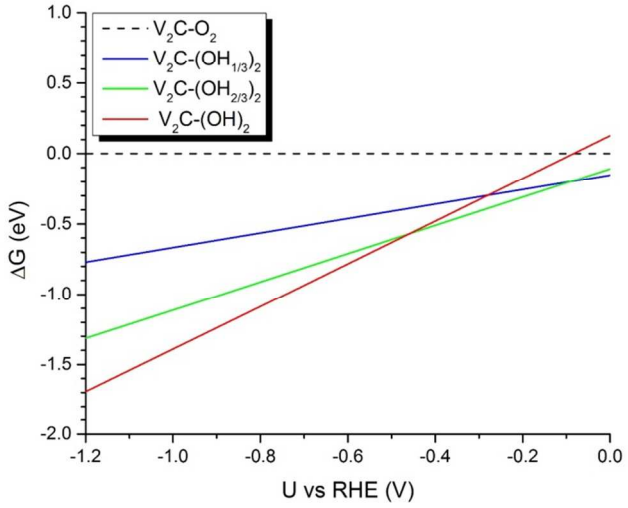

Figure S2. Calculated relative free energies (eV) of different OH coverages (w.r.t. V_2CO_2 and RHE).

U (V)	$V_2C(OH_{1/3})_2$	$V_2C(OH_{2/3})_2$	$V_2C(OH)_2$
0.0	-0.1529	-0.1080	0.1271
-1.2	-0.7698	-1.3121	-1.6938

Table S3. Data used to plot Figure S2.

5. Work function (eV) of MXenes

M_nX_{n+1}	W_{bare} (eV)	W_O	*WHO*	W_F
sc2c	-4.02163	semiconductor	Semiconductor	semiconductor
ti2c	-4.0779	semiconductor	-1.83103	-5.04265
zr2c	-3.91656	semiconductor	-2.07189	-3.98434
hf2c	-4.47168	semiconductor	-2.46955	-3.55996
v2c	-4.56658	-6.6864	-1.76566	-5.52296
nb2c	-4.53881	-5.80539	-2.15064	-4.47982
ta2c	-4.76506	-5.43371	-2.58449	-3.75776
cr2c	-4.69319	-8.00915	Semiconductor	semiconductor
mo2c	-4.58759	-7.39338	-1.81619	-5.73873
ti3c2	-3.81906	-6.15721	-1.8106	-4.98223
v3c2	-4.58157	-6.55148	-1.83023	-5.67346
ta3c2	-4.90524	-5.33699	-2.49638	-4.49258
ti4c3	-3.81747	-6.1264	-2.09035	-4.82451
v4c3	-4.46816	-6.63828	-1.89568	-5.82193
nb4c3	-4.3696	-5.76839	-2.17737	-4.96529
ta4c3	-4.78514	-5.34125	-2.44412	-4.32712
ti2n	-4.54627	-5.9911	-2.1255	-4.6798
zr2n	-4.39661	-4.99367	-2.30219	-3.70032
hf2n	-4.55307	-4.68043	-2.75419	-3.20681
v2n	-4.69187	-6.13505	-1.89944	-5.27783
ti4n3	-4.49034	-5.86673	-2.35257	-4.67932

Table S4. Work function (eV) of MXenes

6. Surface dipole moment density (e/Å) of MXenes

	O	OH	F
sc2c		--	--
ti2c	--	-0.0239	0.00817
zr2c	--	-0.02669	4.88694E-4
hf2c	--	-0.02776	-0.00618
v2c	0.01653	-0.02665	0.00652
nb2c	0.01121	-0.02609	-0.00239
ta2c	0.00522	-0.02561	-0.00733
cr2c	0.01988	--	--
mo2c	0.0187	-0.02796	0.00432

ti3c2	0.01976	-0.0334	0.00388
v3c2	0.02138	-0.02232	0.02122
ta3c2	0.00156	-0.0347	-0.00552
ti4c3	0.02892	-0.05002	0.00984
v4c3	0.02415	-0.04035	0.01501
nb4c3	0.01415	-0.04724	0.00621
ta4c3	0.00667	-0.04805	-0.00263
ti2n	0.01466	-0.02462	0.00183
zr2n	0.00761	-0.02045	-0.00485
hf2n	0.00517	-0.01815	-0.01182
v2n	0.00918	-0.03034	0.00223
ti4n3	0.0198	-0.04569	0.00261

Table S5. Surface dipole moment density (e/Å) of MXenes

7. Formation free energies (eV/T) of surface terminations

	O (0)	OH (0)	F (0)	O (1.23)	OH (1.23)	F (1.23)
sc2c	-2.07321	-2.43849	-3.17374	-4.53321	-3.66849	-4.40374
ti2c	-2.35893	-1.99019	-2.51438	-4.81893	-3.22019	-3.74438
zr2c	-2.90636	-2.16382	-2.7231	-5.36636	-3.39382	-3.9531
hf2c	-3.34228	-2.24923	-2.69881	-5.80228	-3.47923	-3.92881
v2c	-1.50419	-1.31173	-1.74068	-3.96419	-2.54173	-2.97068
nb2c	-1.92688	-1.35809	-1.78263	-4.38688	-2.58809	-3.01263
ta2c	-2.33209	-1.29844	-1.61751	-4.79209	-2.52844	-2.84751
cr2c	-1.09838	-1.01356	-1.46056	-3.55838	-2.24356	-2.69056
mo2c	-1.50958	-0.53261	-0.95134	-3.96958	-1.76261	-2.18134

ti3c2	-2.21363	-1.92019	-2.4598	-4.67363	-3.15019	-3.6898
v3c2	-1.33075	-0.9898	-1.44549	-3.79075	-2.2198	-2.67549
ta3c2	-2.28017	-1.09102	-1.38181	-4.74017	-2.32102	-2.61181
ti4c3	-2.24001	-1.9051	-2.44317	-4.70001	-3.1351	-3.67317
v4c3	-1.30069	-1.03147	-1.47778	-3.76069	-2.26147	-2.70778
nb4c3	-1.68681	-1.08836	-1.5104	-4.14681	-2.31836	-2.7404
ta4c3	-2.13313	-1.05909	-1.3885	-4.59313	-2.28909	-2.6185
ti2n	-2.47362	-1.95239	-2.44429	-4.93362	-3.18239	-3.67429
zr2n	-2.99264	-2.0722	-2.57936	-5.45264	-3.3022	-3.80936
hf2n	-3.34632	-1.99737	-2.34293	-5.80632	-3.22737	-3.57293
v2n	-1.58514	-1.22403	-1.67618	-4.04514	-2.45403	-2.90618
ti4n3	-2.42895	-1.8124	-2.30364	-4.88895	-3.0424	-3.53364

Table S6. Formation free energies (eV/T) of surface terminations

1. Xiao, H.; Tahir-Kheli, J.; Goddard, W. A. *J. Phys. Chem. Lett.* **2011,** 2, 212-217.
2. Crowley, J. M.; Tahir-Kheli, J.; Goddard, W. A. *J. Phys. Chem. Lett.* **2016,** 7, 1198-1203.
3. Xiao, H.; Goddard, W. A. *J. Chem. Phys.* **2014,** 141, 094701.
4. Dovesi, R.; Orlando, R.; Erba, A.; Zicovich-Wilson, C. M., et al. *International Journal of Quantum Chemistry* **2014,** 114, 1287-1317.
5. Monkhorst, H. J.; Pack, J. D. *Phys. Rev. B* **1976,** 13, 5188-5192.
6. Sundararaman, R.; Goddard, W. A. *J. Chem. Phys.* **2015,** 142, 064107.
7. Arias, T. A.; Payne, M. C.; Joannopoulos, J. D. *Phys. Rev. Lett.* **1992,** 69, 1077-1080.
8. Ismail-Beigi, S.; Arias, T. A. *Comput. Phys. Comm.* **2000,** 128, 1-45.
9. Sundararaman, R.; Gunceler, D.; Letchworth-Weaver, K.; Schwarz, K., et al. *JDFTx*.
10. Xiao, H.; Cheng, T.; Goddard, W. A.; Sundararaman, R. *J. Am. Chem. Soc.* **2016,** 138, 483-486.

1. Xiao, H.; Tahir-Kheli, J.; Goddard, W. A. *J. Phys. Chem. Lett.* **2011,** 2, 212-217.
2. Crowley, J. M.; Tahir-Kheli, J.; Goddard, W. A. *J. Phys. Chem. Lett.* **2016,** 7, 1198-1203.
3. Xiao, H.; Goddard, W. A. *J. Chem. Phys.* **2014,** 141, 094701.
4. Dovesi, R.; Orlando, R.; Erba, A.; Zicovich-Wilson, C. M.; Civalleri, B.; Casassa, S.; Maschio, L.; Ferrabone, M.; De La Pierre, M.; D'Arco, P.; Noël, Y.; Causà, Mauro; Rérat, M.; Kirtman, B. *International Journal of Quantum Chemistry* **2014,** 114, 1287-1317.
5. Monkhorst, H. J.; Pack, J. D. *Phys. Rev. B* **1976,** 13, 5188-5192.
6. Sundararaman, R.; Goddard, W. A. *J. Chem. Phys.* **2015,** 142, 064107.

7. Arias, T. A.; Payne, M. C.; Joannopoulos, J. D. *Phys. Rev. Lett.* **1992,** 69, 1077-1080.
8. Ismail-Beigi, S.; Arias, T. A. *Comput. Phys. Comm.* **2000,** 128, 1-45.
9. Sundararaman, R.; Gunceler, D.; Letchworth-Weaver, K.; Schwarz, K.; Arias, T. A. *JDFTx*, available from http://jdftx.sourceforge.net (2012).
10. Xiao, H.; Cheng, T.; Goddard, W. A.; Sundararaman, R. *J. Am. Chem. Soc.* **2016,** 138, 483-486.